Regenerative Engineering and Translational Medicine
https://doi.org/10.1007/s40883-025-00442-9

ORIGINAL RESEARCH

Influence of Reinforcement Material on Fatigue Features of Trans-Tibial Prosthetic with Epoxy Matrix

Noor K. Faheed[1] · Mahmood S. Mahmood[2] · Rasha A. Issa[3] · Qahtan A. Hamad[4] · Dheyaa S. J. Al-saedi[5]

Received: 26 June 2024 / Revised: 30 April 2025 / Accepted: 20 May 2025

Abstract
When new manufacturing techniques, materials, and socket designs are introduced, prosthetic limb consumers may need them since the corpus of knowledge currently available for safe fabrication may no longer be relevant. In this paper, the authors investigated the influence of dynamic and cyclic loading on the resulting damage and its propagation in natural fiber–reinforced polymeric composites utilized in trans-tibial prosthetic sockets experimentally, numerically, and theoretically. Using epoxy as the matrix and reinforcements such as perlon, rami, coir, pineapple, glass, and carbon, six groups were formed using vacuum pressure. The materials used in the socket above underwent tensile and fatigue testing. Using a finite element method, the theoretical section calculated the failure index, fatigue life, volume fraction, and theoretical safety factor. The experimental findings allowed us to assess fracture mechanisms during this loading. In addition to the viscoelastic properties, the kind of reinforcement significantly influences the observed parameters. This study thoroughly examined the criteria for natural fiber–reinforced polymer composites for prosthesis purposes, emphasizing efficiency, structural performance, environmental effects, financial considerations, and safety factors. The suggested natural fiber–reinforced (NFR) composites are a practical and environmentally beneficial alternative since they satisfy safety and performance requirements. NFR composites are positioned to significantly influence how biomedical engineering is produced in the future as sustainability becomes a major design and production priority.

Lay Summary Amputees have yet to utilize prosthetic sockets composed of natural fibers, despite their potential to be created from traditional sources. This study successfully designed and evaluated a new prosthetic socket that employs biocompatible and sustainable components to lower the prosthesis's weight and associated expenses while retaining durability under cyclic loads.

Keywords Fatigue · Coir · Pineapple · Rami · Polymer composite · Prosthesis

Introduction

A prosthesis is a synthetic item that replaces a missing organ, including a limb, teeth, eye, or heart valve. Prostheses are frequently utilized to reclaim the appearance and lost functions of patients with amputations. According to the World Health Assembly, 35–40 million people need assistance, aids, and services for prosthetic and orthotic purposes [1].

The seriousness of the condition determines the extent of amputation. When resection of the lower limb extends

✉ Noor K. Faheed
noor.kf@uomisan.edu.iq

Mahmood S. Mahmood
mahmood-shacker@uomisan.edu.iq

Rasha A. Issa
rasha.a.issa2@gmail.com

Qahtan A. Hamad
qahtan.a.hamad@uotechnology.edu.iq

Dheyaa S. J. Al-saedi
diaa.sabeeh@uomisan.edu.iq

[1] Department of Chemical Engineering, College of Engineering, University of Misan, Amarah, Misan, Iraq

[2] Department of Mechanical Engineering, College of Engineering, University of Misan, Amarah, Iraq

[3] Ministry of Higher Education and Scientific Research, Baghdad, Iraq

[4] Materials Engineering Department, University of Technology - Iraq, Baghdad, Iraq

[5] Department of Petroleum Engineering, College of Engineering, University of Misan, Amarah, Misan, Iraq

Published online: 04 June 2025

past the ankle, below-knee (BK) amputation is employed. When there is proximal illness or negligible wound repair following the BK amputation, the above-knee (AK) resection is often carried out as a follow-up procedure. The benefits of AK amputation involve a bearing weight stump at the extremity, improved stability because of the retention of the adductor muscle's insertion [2, 3], streamlined prosthetic instrument development due to fewer articulations [4, 5], lowering the effort needed to swing a limb when strolling, and assisting with sitting equilibrium and moving from bed to chair. Furthermore, increased rehabilitative capacity and improved postoperative quality of life have been documented [4].

A prosthetic socket is an important prosthesis component because it links the remaining limb to the prosthetic apparatus. As a result, it must be developed and manufactured to ensure proper fit and ease of use. At the same time, a lower-limb prosthesis socket is subjected to numerous loads owing to the amputee's body weight and motion. As a result, evaluating the functionality of a socket is critical to ensuring adequate durability and strength [1]. The artificial lower limb socket must be built to withstand the forces that walking will inflict on the prosthesis. Furthermore, the design should be adjusted to appropriately transmit these stresses to parts of varying stiffness, thereby protecting stiffer tissues from high pressure and reducing undesirable relative motion induced by soft tissue compressing. The market need for lower limbs has expanded in quality and quantity [5].

The behavior and endurance characteristics of elements composed of polymeric composites that are exposed to cyclic stress may be significantly impacted by dissipation mechanisms. The majority of the energy lost during this procedure is converted to heat. The self-heating phenomenon is initiated when heat created during extended cyclic deformations is retained inside the material, and the temperature rises due to the limited thermal conductivity of most polymers employed in engineering applications. In addition, thermal cycling may result in individual fiber layers breaking or the composite delaminating [6].

The advancement of industrial technology has resulted in a growing need for commercial supplies with specific qualities. Consequently, novel materials with unique features are constantly in demand, and as a result, new disciplines of composite materials have emerged, particularly in the past 20 years. The composites have numerous key mechanical features, rendering them ideal for various industrial applications. Polymer composites are widely employed in high-tech applications such as prosthetics, the aerospace industry, automobiles, and sporting goods [7, 8]. The predominant prosthetic sockets are fabricated from monolithic thermoplastic polymers like polypropylene (PP), which are deficient in durability and strength and demonstrate creep, prompting the adoption of composite materials [9]. Fiberglass and carbon are likely the most frequent and inexpensive reinforcements among the traditional fibers employed in these composites. Despite being one of the thickest fibers, it is easy to soak in resin and offers a variety of applications and qualities [10].

Various researchers have utilized fibers from plants, such as ramie, flax, pineapple, cotton, and banana, to make bio-based combinations to solve the problems of pricey composites derived from artificial fibers [11, 12]. Nowadays, there are several benefits to using natural fibers as reinforcements in composites, including a decrease in materials made from non-renewable resources and a less negative impact on the environment. These materials have been successfully used as hydrogels, scaffolding, matrices, implantation, and delivery of drugs, tissue engineering, wound healing, and nanotechnology [13]. Because the fibers are derived from renewable resources, the reinforcements were injected with either epoxy or polyester polymer to create bio-composites. In addition, several natural fiber–strengthening materials lack the rigidity and strength required to keep the limb in place during prosthetic usage. To address this problem, hybrid materials containing natural fibers and artificial (glass, carbon, and perlon) were developed [14, 15].

Despite the advancement of natural materials from traditional resources, natural fiber–laminated materials have yet to be used in prosthetic sockets for amputees engaged in dynamic movements [16].

Numerous investigations have been conducted to find acceptable composite substances for socket manufacturing. Al-Khazraji et al. investigated the fatigue and tensile characteristics numerically, theoretically, and experimentally. To make efficient prosthetic sockets for the lower limbs, the matrix material of these composites was strengthened with woven fibers and particles, including perlon, glass, carbon, and hybrid (carbon and glass) silica nanoparticles. The findings demonstrate that altering the kind of reinforcement significantly affects the measured parameters [17]. Sattar M. A. et al. investigated ideal composite materials, particularly concerning fatigue loading resistance, for through-knee (TK) prostheses. Fabrics made of carbon, perlon, and fiberglass make up the reinforcement. Tensile, fatigue, and bending tests were among the mechanical tests used to evaluate the durability of these laminates. The findings demonstrated that TK prostheses can enable better socket fitment practices and the development of customized prostheses specific to the patient's sockets [18]. Oleiwi et al. investigated lamination groups with varying layering combinations using tensile testing to examine the impacts of using hybrid fibers and adding more layers in an experimental, theoretical, and numerical approach. In addition to enabling the production of high-performance biocomposites by integrating natural and artificial reinforcement, the study revealed that the quantity and kind of fibers affected mechanical qualities.

The theoretical and experimental results were in agreement with the FEM results [19]. Afroza Khatun et al. studied the physical, mechanical, and thermally processed degradation and morphological properties of hybrid composites reinforced with palmyra palm fiber and date palm fruits. Tensile, weight, water absorption, FTIR, SEM, DSC, and thermogravimetric evaluation (TGA) were used to achieve this. Compression molding was used to make the composites at different weight percentages (5, 10, 15, 20, and 25 wt.%) of fiber volume. According to analyses, composite hybrids with 5% fiber volume have the best-achieved properties [20]. Appadurai et al. produced sockets that are used in a knee prosthesis. An 80:20 resin blend of perlon, carbon, Kevlar, and fibers from Kenaf was employed to achieve the greatest effectiveness. This material can be utilized to construct structures with a suitable design, adequate mechanical qualities, and long-term endurance. The samples were subjected to tensile, bending, and shock testing [21].

For the prosthetic to function as best it can, the socket must be able to move. Any motion between the remaining limb and the socket will make successful ambulation challenging, leading to pain and exhaustion. This is because the forces generated by the remaining limb throughout gait movement must be appropriately transferred from the limb to the prosthetic. A well-known phenomenon in material fatigue is that even when the maximum stress is lower than the proof or yield stress, many stress fluctuations at a single location can produce rupture. Tensile stress at a macro or micro defect causes the fracture. Patients desire the best possible fit, maximum comfort, and maximum effectiveness from their prosthetics. The prosthesis also needs to be visually appealing and portable. During cyclic walking stresses, nearly all prosthetic malfunctions are fatigue-related.

This article examines how material type affects trans-tibial prosthetic sockets' tensile and fatigue properties (S–N curve, strain energy-N, and fatigue limit). It does this by measuring the structural strength of the socket using experimental, numerical, and theoretical methods for six different reinforcements (perlon, carbon, glass, coir, rami, and pineapple fibers) using epoxy polymer as a matrix. The goal is to determine the best candidate to improve the fatigue characteristics of the trans-tibial prosthetic socket and the ideal combination of reinforcement and matrix fibers.

It was determined that the composites (pineapple with carbon reinforcements) may provide inexpensive and long-lasting prostheses by producing the best experimental, numerical, and theoretical findings, making it the most likely option to enhance the trans-tibial prosthetic socket's fatigue and mechanical properties. This evaluation provided extensive information, covering the most current material advances, particularly the impact of natural fiber–reinforced composites for prosthetic uses. This could enable readers to identify several untapped possibilities that could help invent novel and innovative technologies in this area of research.

Methods

Experimental Methodology

The research's experimental methodology comprised as follows.

Materials

The following materials are utilized in the production of AK prosthetics and orthopedic devices: glass-woven fabric (element health care 616G3), Perlon-woven fabrics stockinet white (element label is (623 T5), carbon-woven fabrics (unidirectional reinforcements that are woven where all fibers seriatim in a single, parallel path), epoxy polymer (consider Supreme for producing lightweight yet extraordinarily durable orthoses and prostheses), hardening powder (Health Care item 617P37), and both outer and inner adaptable polyvinyl acetate (PVA) bags. Otto Bock's business provided all the materials above.

Rami fiber, coir fiber, and pineapple fiber (as a woven mat produced by Changzhou Doris Textiles Co., Ltd.) were immersed in a 5% sodium hydroxide solution for approximately 2 h at ambient temperature. This improved the mechanical properties of preparing high-performance natural fiber composite boards by increasing the fibers' tensile strength, longevity, and attraction to the matrix. They were extensively cleaned under running water after the alkalization process.

Equipment Utilized in This Study

The equipment involves a gypsum mold that creates rectangular specimens with 20, 26, and 5 cm^3 dimensions; the engine and holder for the mold structure are the mechanisms for discharging the captured pressure and air, mechanical factories where samples are made, cut, and assembled. A CNC cutting instrument cuts the samples to the requisite dimensions. These workshops also handle the assembly of prosthetic limb elements in addition to equipment for fatigue and tensile testing of samples.

Sample Preparation for Testing

Composite laminated groups were created using the vacuum-bagging technique. To prevent the formation of bubbles inside the specimens, the mold was tightly attached and linked to pressure vacuum devices, with the link made via

Fig. 1 **A–D** The different stages of samples' fabrications

Table 1 Groups utilized in laminations

No. of lamination	Lamination lay-up	Name	Lamination lay-up procedures
Lamination 1	4 perlon + 3 coir + 2 carbon	(COC)	(2P + 1 CO + 1 C + 1 CO + 1 C + 1 CO + 2P) layers
Lamination 2	4 perlon + 3 coir + 2 fiber glass	(COG)	(2P + 1 CO + 1G + 1 CO + 1G + 1 CO + 2P) layers
Lamination 3	4 perlon + 3 rami + 2 carbon	(RC)	(2P + 1R + 1 C + 1R + 1 C + 1R + 2P) layers
Lamination 4	4 perlon + 3 rami + 2 fiber glass	(RG)	(2P + 1R + 1G + 1R + 1G + 1R + 2P) layers
Lamination 5	4 perlon + 3 pineapple + 2 carbon	(PIC)	(2P + 1Pi + 1 C + 1Pi + 1 C + 1Pi + 2P) layers
Lamination 6	4 perlon + 3 pineapple + 2 fiber glass	(PIG)	(2P + 1Pi + 1G + 1Pi + 1G + 1Pi + 2P) layers

pipes, as illustrated in Fig. 1A. The PVA layer was positioned on the mold to aid in insulating the fibers soaked with the matrix from the mold and prevent it from sticking, and then pressure taps were released to 40 kPa at room temperature. Reinforcement layers were applied as illustrated in Table 1. A sheet of PVA bag was placed above the composite material layers. According to the manufacturer's guidelines, the epoxy resin was mixed with hardening powder and injected into the mold. Figure 1B, C illustrates that the silicone string closed the bag. After an hour, the completed composite specimen was removed and cut with an electrical saw. Figure 1D shows the process we used to cure composite laminates from various fabrics. The appropriate volume fractions were calculated using the reinforcement and matrix weights.

The method of production used in this study ensures that fiber orientations in a laminate are evenly distributed; the material's strength and stiffness remain consistent irrespective of the direction of the load. This is known as quasi-isotropic characteristics.

Tensile Test

This test was critical in gathering the mechanical properties needed as the data needed for the numerical analysis. A stress–strain curve was acquired for every sample by employing the tensile test. It is applied to evaluate tensile features, such as ultimate tensile strength (UTS), elastic modulus (E), and specific strength and modulus values at the break for these samples. This test is carried out following

ASTM D638 at ambient temperature with a 5 kN load and a strain rate of 1 mm/min [22].

Eighteen standard samples were constructed in the present investigation. The University of Technology's Materials Division conducted the test using a testing apparatus from Instron, and the load was maintained until the break happened.

Fatigue Test

Alternate bending fatigue with a steady amplitude is a fatigue testing apparatus. One side of the samples was fixed while the other was exposed to flexion perpendicular to the samples' axis, resulting in bending stresses.

The fatigue test may fail when a flat sample breaks under alternate loading. The University of Technology's Materials Division conducted the test using a cyclic fatigue testing device (HSM20, 1400 rpm, 230 V voltage, 20 Hz frequency, 0.4 kW power) at ambient temperature with a stress ratio of $R = 1$. The machine's handbook depicts the fatigue standards sample test in Fig. 2 [23].

Finite Element Analysis (FEM) Numerical Analysis

The finite element methodology, which takes advantage of the quick advancement of computer systems with high memory capacities and fast computing, is currently widely employed in many scientific and engineering domains. The method's abilities, encompassing complicated geometrical constraints and non-linear material characteristics, have made it one of the most potent numerical techniques [24]. Three separate processes make up the ANSYS analysis: simulating the socket's design in the initial stage, classifying the load and finding a solution in the second stage, and evaluating the outcomes in the third stage [25, 26].

To study the patients' motion mechanisms, the socket architecture was split into four fundamental groups (anterior, posterior, lateral, and medial) depending on their bearing weight characteristics. Next, while each patient moved at a pace that they chose for themselves, interface pressures across the residual leg and the socket were recorded [27].

Utilizing the ANSYS program, the numerical method assessed the definitions of fatigue of substances used for prosthetic production. First, the model specimen for composite materials had to be meshed. Next, the fatigue characteristics of the material were assessed by inputting the mechanical characteristics of the composites, which were reviewed through an experimental approach [28, 29].

The modeled prosthetic socket's dispersion is provided using the finite element method for the following parameters: equivalent alternating, maximum shear stress, and total deformation, fatigue life, and safety factor. The socket model assessed the numerical characteristics as the boundary condition. As seen in Fig. 3, the boundary condition was imposed as a fixed base at the lower surface, more precisely, at the bottom point of the socket. The load utilized by the ANSYS® Workbench program will be set at the socket adapter. As seen in Fig. 3, the interface pressure is dispersed based on specific places.

This work uses finite element modeling with ANSYS® Workbench 16 technology as a numerical instrument to show how pressure and deformation affect a structural component and how the suggested bidirectional woven fabric-strength model behaves. The model was constructed on a 25-year-old man who weighed 77 kg and had been amputated above the knee. The procedure is classified as a lengthy above-knee amputation because of the 26 cm length of the stump. A three-dimensional socket model is created based on the precise geometrical measurements of the amputee stump, as demonstrated in the example given in reference [31]. The model is tested at the most dangerous load conditions throughout the heel contact gait cycle. Data were arranged in a layered pattern on the socket planes in Fig. 3, according to pressure. The tensile test yields the mechanical characteristics of the groups used, and the law of mixture is used to calculate density and Poisson's ratio, as indicated in Table 2

Fig. 2 Two sets of natural fiber specimens before the test

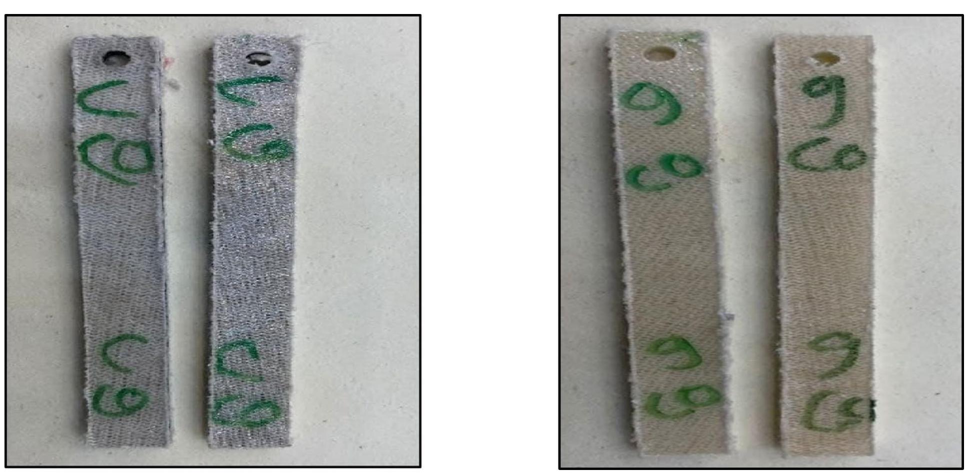

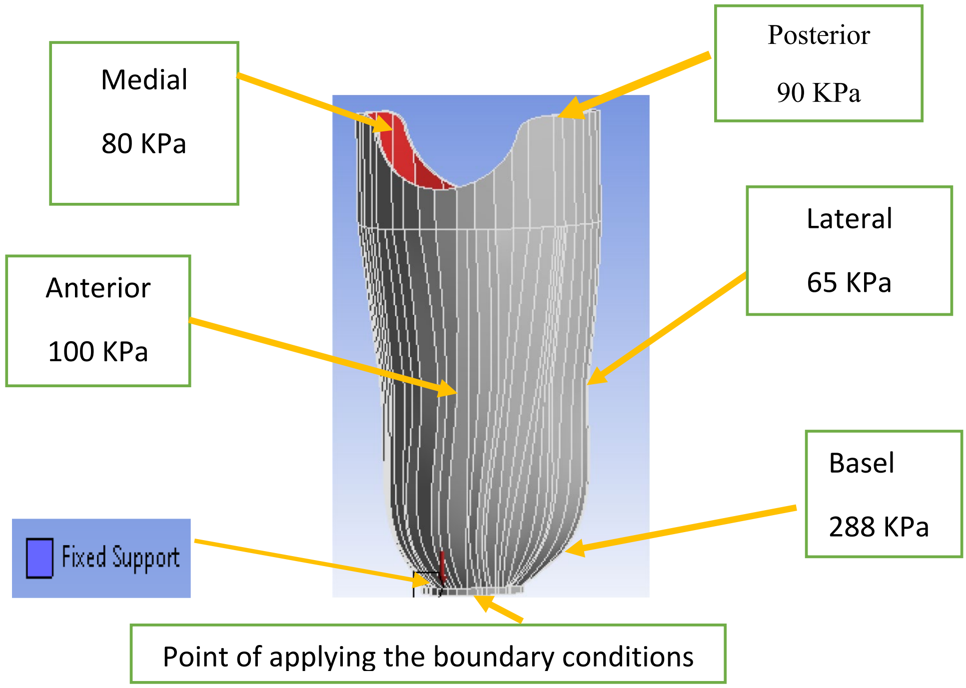

Fig. 3 Position of applied pressure and boundary conditions [30]

Table 2 Characteristics of the composites employed

Lamination	Density (g/cm^3)	Poisson's ratio	Yield strength (MPa)
COC	**1.233**	**0.335**	**140**
COG	**1.276**	**0.272**	**83**
RC	**1.125**	**0.341**	**41**
RG	**1.134**	**0.332**	**60**
PIC	**1.225**	**0.321**	**420**
PIG	**1.266**	**0.277**	**172**

[27, 28]. The meshing process was finished by choosing the volume and setting the model's character to "automatic meshing," as seen in Fig. 4. Interaction pressure was applied at specific positions. As seen in Fig. 4, this mesh includes 8935 elements and 18,138 nodes, providing various ANSYS features and a node count.

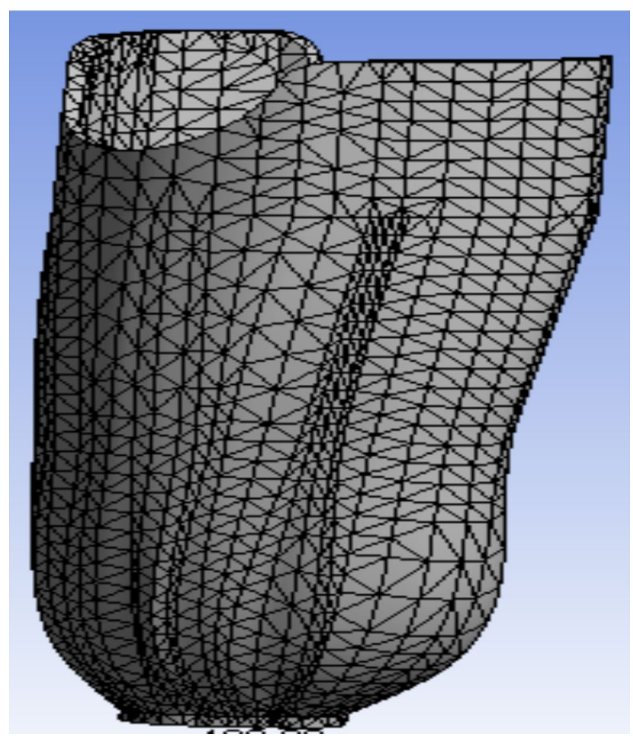

Fig. 4 The meshed artificial socket

Theoretical Part

The theoretical section of the piece is based on the ideas and concepts listed below.

Goodman Relationship

The correlation between the mean stress and fatigue limit has been described via empirical relations [32]:

$$\frac{\sigma_a}{\sigma_e} + \frac{\sigma_m}{\sigma_{ts}} = 1 \tag{1}$$

where:

$a$von Mises equivalent stress or stress amplitude.
$e$endurance limit stress.
$m$mean stress.

Fatigue Ratio (Rf)

The proportion of the tensile stress to the endurance limit is known as the fatigue ratio (Rf) [33]:

$$FatigueRatio(R_f) = \frac{Endurancelimit(\sigma_e)}{TensileStrength(\sigma_{ts})} \tag{2}$$

Safety Factor (SF)

An effective engineering design must always take safety into account. It aims to consider factors at every engineering design and production stage. The degree to which the safety variables vary depends on the condition [30].

Failure within the design period is indicated when the stress in a specific location of the model exceeds the material's strength limitation [34]. This increases the likelihood that the stress in a particular area of the model will go beyond the material's strength limit. The following formula can be used to determine the theoretical safety factor.

$$Theoreticalsafetyfactor = (ExperimentalFailurestrength)/(vonMisesstress) \tag{3}$$

Failure Index (K)

One of the most important design criteria for composite structures is failure analysis. Several requirements have been proposed to predict composite failure. The probable failure areas for the composite laminate design are displayed by the scalar quantity known as the failure index. The failure index can be positive or negative. You should have a failure index with a value below 1. The layers may fail in regions where the failure index is higher than 1 [35].

The failure index, or the percentage of vonMises stress to investigate failure strength, can be computed using Eq. (4) [36]:

$$FailureIndex(k) = (vonMisesStress)/(ExperimentalFailurestrength) \tag{4}$$

Table 3 Physical assets of the composites of this research

Lamination	Thickness (mm)	Volume fraction %
COC	**4.3**	**29.27**
COG	**4.4**	**51**
RC	**2.4**	**26.31**
RG	**3**	**27**
PIC	**3.7**	**35.1**
PIG	**4**	**46.8**

Results, Discussion, and Implications

Experimental Results

Physical Characteristics of Specimens

Electronic Vernier and weighing devices estimate the samples' weight and thickness, and the law of mixture computes the volume fractions [36, 37]. The weights were determined using Archimedes' approach, and the density was determined using the ASTM (D-792 standards).

Table 3 illustrates the effect of prosthetic socket reinforcement on average thickness. Nevertheless, none of the reinforcing materials significantly differed. The heaviest type of reinforcing is hybrid (coir glass), while hybrid (rami carbon) was the thinnest [38, 39].

Table 3 compares volume fractions with various reinforcing materials and layer numbers. The uppermost volume fraction is instituted in the coir glass strengthening samples, while the lowest volume fraction is obtained with the rami and carbon lamination group. Changing the type of reinforcements and increasing the number of fiber layers boosts the absorption capacity. The fiber volume fraction results validated our analysis [40].

Fatigue Test Results

In this study, the six lamination groups underwent fatigue testing. The fatigue tester's findings disclosed the intervals

Fig. 5 Experimental fatigue stress of epoxy matrix reinforced with coir fiber reinforcement

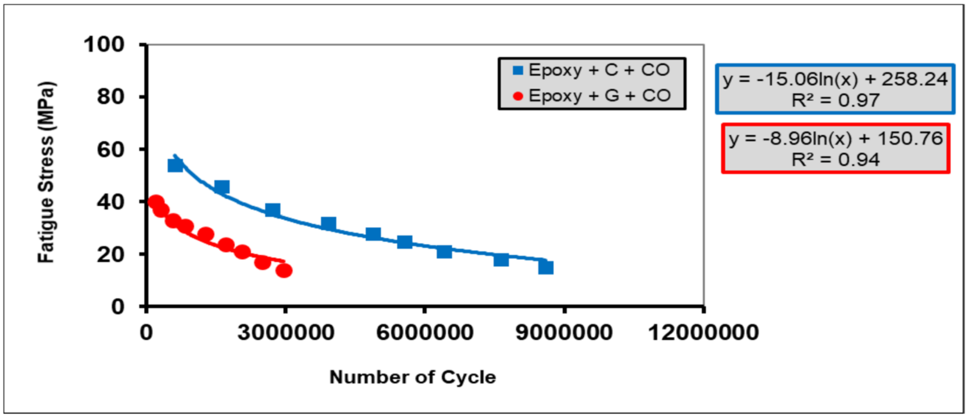

Fig. 6 Experimental fatigue stress of epoxy matrix reinforced with pineapple fiber reinforcement

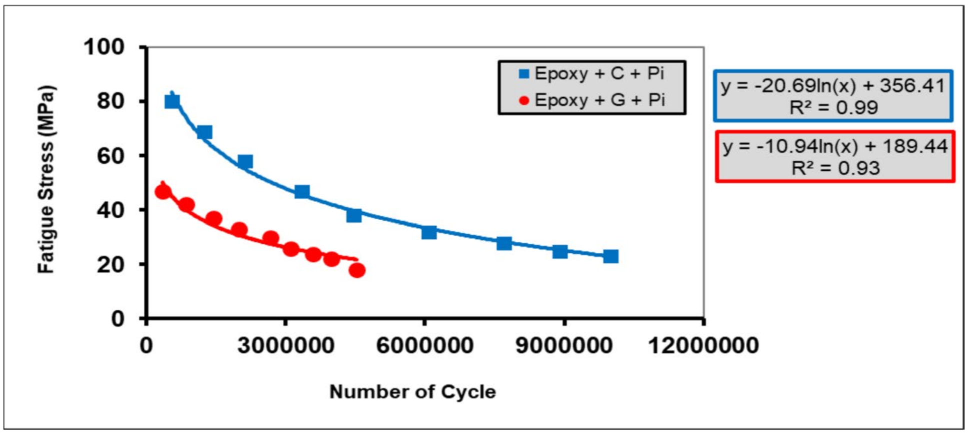

Fig. 7 Experimental fatigue stress of epoxy matrix reinforced with rami fiber reinforcement

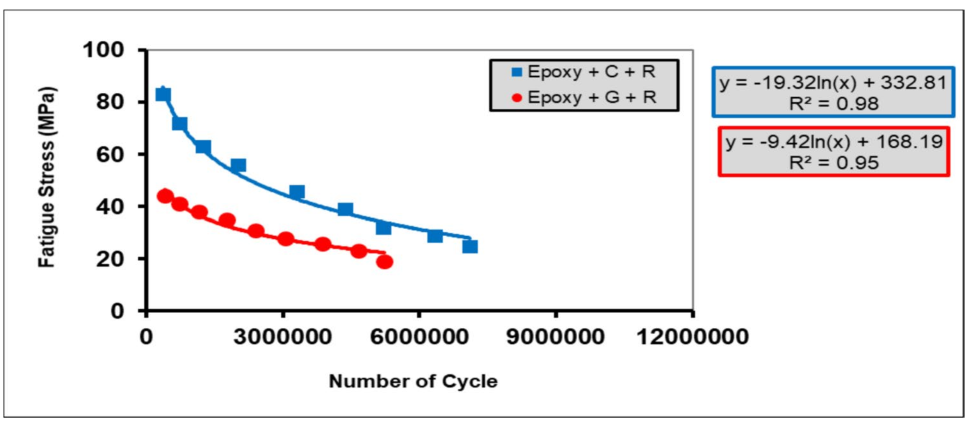

needed to break the samples. Drawing a curve representing the results of experiments from fatigue tests yields the fatigue S–N curve [41, 42]. The testing fatigue stress of the specimens, along with the number of cycles at which the fracture occurred from each lamination, are displayed in Figs. 5, 6, and 7. The instruments used to test for fatigue revealed that the number of repetitions in fatigue failure increases as fatigue failure stress decreases, suggesting that using hybrid materials can change fatigue life and strength. These curves are attained by fitting the fatigue test's experimental statistics, utilizing the logarithmic method [18].

The fatigue limit, also known as the endurance limit, is the stress level below which a material can withstand an infinite number of loading cycles without failing due to fatigue. It was discovered by testing samples to establish the maximum stress at which the material does not fracture after a predetermined number of cycles [34].

Figure 8 demonstrates the kinds of reinforcements and their fatigue limits. The elastic modulus of rami fiber

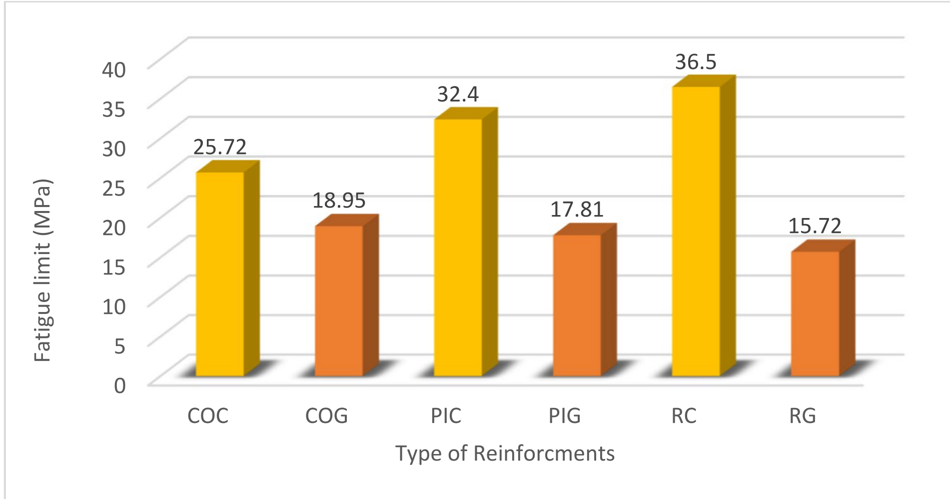

Fig. 8 Fatigue limit of epoxy matrix composite with different reinforcements

Table 4 Statistical analysis of fatigue test

Groups		*N*	Mean	Std. deviation	Std. error	Minimum	Maximum	*P*-value between groups
Epoxy + Co + C	1	3	54.00	2.000	1.155	52	56	.000
	2	3	46.00	2.646	1.528	43	48	(VHS)
	3	3	37.00	2.000	1.155	35	39	
	4	3	32.00	2.646	1.528	29	34	
	5	3	28.00	4.359	2.517	25	33	
	6	3	25.00	5.568	3.215	19	30	
	7	3	21.00	2.646	1.528	19	24	
	8	3	18.00	2.646	1.528	15	20	
	9	3	15.00	2.000	1.155	13	17	
Epoxy + Co + G	1	3	40.00	3.000	1.732	37	43	.000
	2	3	37.00	2.646	1.528	35	40	(VHS)
	3	3	33.00	1.000	.577	32	34	
	4	3	31.00	1.000	.577	30	32	
	5	3	28.00	1.000	.577	27	29	
	6	3	24.00	1.000	.577	23	25	
	7	3	21.00	1.000	.577	20	22	
	8	3	17.00	1.000	.577	16	18	
	9	3	14.00	1.000	.577	13	15	

reinforcements differed from that of coir and pineapple reinforcements, leading to better fatigue performance. This may be explained by the bonding strength's character and the enhancing process, which provides seamless contact between the matrix and the reinforcing materials [43].

Notably, the fatigue properties of natural fibers were enhanced by adding glass and carbon fibers, with the carbon fiber showing a modification of the fatigue performance of composite materials. Rami hybrid specimens can support greater loads because carbon fibers have a better modulus of elasticity and resilience to crack development than the matrix material. A material's fatigue strength depends on how stiff it is. As stated, materials possessing a greater modulus of elasticity also exhibit greater fatigue strength [44].

Generally, the fatigue limit is proportionate to their tensile strength; henceforth, materials with greater ultimate tensile strength retain a greater fatigue limit [45]. Lamination for RC has a superior fatigue life, as can be seen. These findings showed that the recommended model's fatigue strength was greater than the other laminations [43].

Tables 4, 5, and 6 show the descriptive statistics (std. error, std. deviation, minimum, mean, and maximum) and one-way ANOVA (p-value across groups) for the fatigue strength test. The findings were statistically assessed utilizing one-way

Table 5 Statistical analysis of fatigue test

Groups		N	Mean	Std. deviation	Std. error	Minimum	Maximum	P-value between groups
Epoxy + Pi + C	1	3	80.00	3.606	2.082	77	84	.000
	2	3	69.00	2.000	1.155	67	71	
	3	3	58.00	2.000	1.155	56	60	
	4	3	47.00	2.646	1.528	44	49	
	5	3	38.00	2.000	1.155	36	40	
	6	3	32.00	2.646	1.528	29	34	
	7	3	28.00	1.000	.577	27	29	
	8	3	25.00	2.000	1.155	23	27	
	9	3	23.00	2.000	1.155	21	25	
Epoxy + Pi + G	1	3	47.00	2.000	1.155	45	49	.000
	2	3	42.00	1.000	.577	41	43	(VHS)
	3	3	37.00	2.000	1.155	35	39	
	4	3	33.00	3.000	1.732	30	36	
	5	3	30.00	3.000	1.732	27	33	
	6	3	26.00	2.000	1.155	24	28	
	7	3	24.00	1.000	.577	23	25	
	8	3	22.00	2.000	1.155	20	24	
	9	3	18.00	1.000	.577	17	19	

Table 6 Statistical analysis of fatigue test

Groups		N	Mean	Std. deviation	Std. error	Maximum	Minimum	P-value between groups
Epoxy + R + C	1	3	83.00	2.000	1.155	81	85	.000
	2	3	72.00	2.000	1.155	70	74	(VHS)
	3	3	63.00	2.000	1.155	61	65	
	4	3	56.00	2.000	1.155	54	58	
	5	3	46.00	3.606	2.082	43	50	
	6	3	39.00	1.000	.577	38	40	
	7	3	32.00	3.000	1.732	29	35	
	8	3	29.00	2.646	1.528	27	32	
	9	3	25.00	1.000	.577	24	26	
Epoxy + R + G	1	3	44.00	2.000	1.155	42	46	.000
	2	3	41.00	2.000	1.155	39	43	(VHS)
	3	3	38.00	4.000	2.309	34	42	
	4	3	35.00	5.000	2.887	30	40	
	5	3	31.00	2.646	1.528	28	33	
	6	3	28.00	2.000	1.155	26	30	
	7	3	26.00	2.000	1.155	24	28	
	8	3	23.00	1.000	.577	22	24	
	9	3	19.00	2.000	1.155	17	21	

ANOVA in SPSS. Given that fatigue stress is usually linked to tensile load, the results showed that the mean values of fatigue stress for the laminated groups strengthened with rami and pineapple fibers were higher than those for coir fiber. The increased tensile strength may explain this [44]. Furthermore, the RC group's fatigue stress (83 MPa) was greater than that of the glass-fiber-reinforced group (44 MPa). The cavitation mechanism, which causes the rubbery mix particles close to the crack tip to expand and absorb a large portion of the energy, is responsible for these greater fatigue characteristics, boosting fracture toughness. This may help explain the differences between the RC and RG groups because of the improved mechanical properties of adding these reinforcements, which have greater strength and improved contact with the epoxy matrix [8]. A difference (VHS) ($p \leq 0.001$) has been observed between the groups and the coir fiber–strengthened laminated groups.

Numerical Results

Fatigue Life Results

The numerical fatigue life calculations for the different composites with different reinforcement components are displayed in Fig. 9A, B. The possible life for a specific fatigue analysis is shown as fatigue life. The fatigue response of composite materials modified by rami fiber reinforcement, as seen in Fig. 9A, was higher than that of composite materials modified by strengthened coir or pineapple fibers, achieving a maximum value with laminate (RC) of 10.5 MPa. This finding may indicate adequate bonding among the fibers and matrix, where fatigue characteristics can be enhanced by applying an alkaline treatment [46]. It is clear that the kind of reinforcement significantly affects the resilience to fatigue of all laminate groups. Coir fiber–based composites have a lower fatigue life because these fibers typically have poor tensile strength and stiffness due to less cellulose and hemicellulose. Furthermore, poor bonding contact between the polymer and fibers in the matrix might clarify the variance between the CCO and COG groups [47].

Counterplots displayed the general dispersion of life across the socket for every composite utilized in this investigation, as illustrated in Fig. 9B. The life at that level will be considered in stress life assessment with a constant magnitude if the equivalent alternating stress is less than the minimum alternating stress determined by the curve of S–N curve [22].

Fatigue Factor of Safety Results

The static analysis results serve as the primary foundation for the fatigue assessment. The maximal stress encountered in fatigue analysis, which allows one to determine how long the prosthetic socket will tolerate fatigue stressors by calculating the load factor, is known as the principal stress [48].

The minimum safety factor for every composite is shown in Fig. 10A, where it is evident that the composites with the lowest safety factors were 0.882, 3.36, and 5.46, respectively, that were the pineapple with carbon reinforcement, the coir with glass reinforcement, and the coir with carbon reinforcement. Since every material has reached maximum safety factor values equal to 15, guaranteeing that failure will not occur before the design life has been met, all materials are considered safer composites, and this could be attributed to the fibers possessing greater mechanical requirements than the matrix. In addition, the volume fraction of the fibers inside the cross-sectional area rises due to an alteration in the reinforcement kind and the addition of more layers [49, 50]. The general distribution of the composite's secure and risky areas safety factor across the prosthetic socket for the material utilized in this investigation was shown using a counterplot (Fig. 10B).

Equivalent Stress (von Mises Analysis Stress) Results

Thanks to the von Mises stress assessment, we were able to determine the quantity of stress created and comprehend how the stress spread throughout the socket. Equivalent alternating stress, after considering fatigue loading form, R-ratio impacts, and additional fatigue analysis variables, is used to construct the fatigue S–N curve for numerical evaluation. The last number determining the fatigue life is equivalent to alternating stress [49].

Figure 11A displays the outcomes of correlating the equivalent von Mises stress produced for the composites. Maps of contours depicting the general distribution of von Mises stress and the estimated location and size of the severe von Mises stress are shown in Fig. 11B. The results indicate that the highest stress generated in the socket is 26.21 MPa at the center of the anterior portion of the tibia bone; however, the posterior, lateral, and medial portions contribute to a lower pressure than the anterior portion. Hybrid (rami carbon) displayed the highest equivalent stress with (26.212 MPa), and the increase could be attributed to carbon and rami fibers' high strength and stiffness. Meanwhile, lamination (coir + glass) layers and medial and lateral portions created the lowest equivalent stress (25.57 MPa) [50].

Maximum Shear Stress Results

Figure 12A presents the maximum shear stress for each of the six kinds of lamination models. At the center of the anterior region of the tibia bone, the highest shear stress generated by the socket is 14.008 MPa for the (rami + carbon) lamination group due to having a greater resistance to bending than the matrix. However, Lamination 1 (2Perlon + 1 Coir + 1 Carbon + 1 Coir + 2Perlon) layers have the lowest equivalent strain (13.5 MPa), whereas the medial, posterior, and lateral sections contribute to pressure that is less than the anterior part [51].

Figure 12B shows each of the six composites' contour plots, illustrating the maximum shear stress's general distribution across the material and its probable position and

Fig. 9 **A** Numerical results of composites fatigue life. **B** Specimens of contours of laminations fatigue life

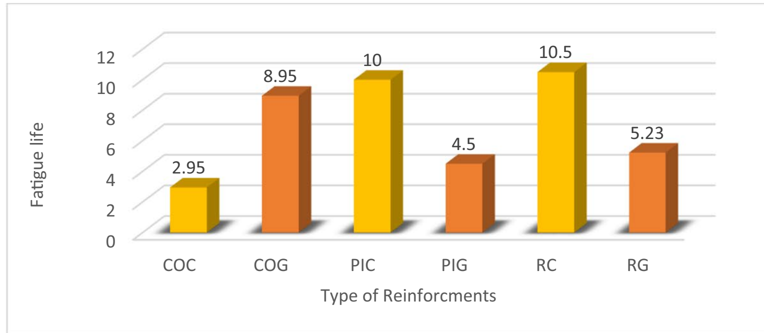

(A)

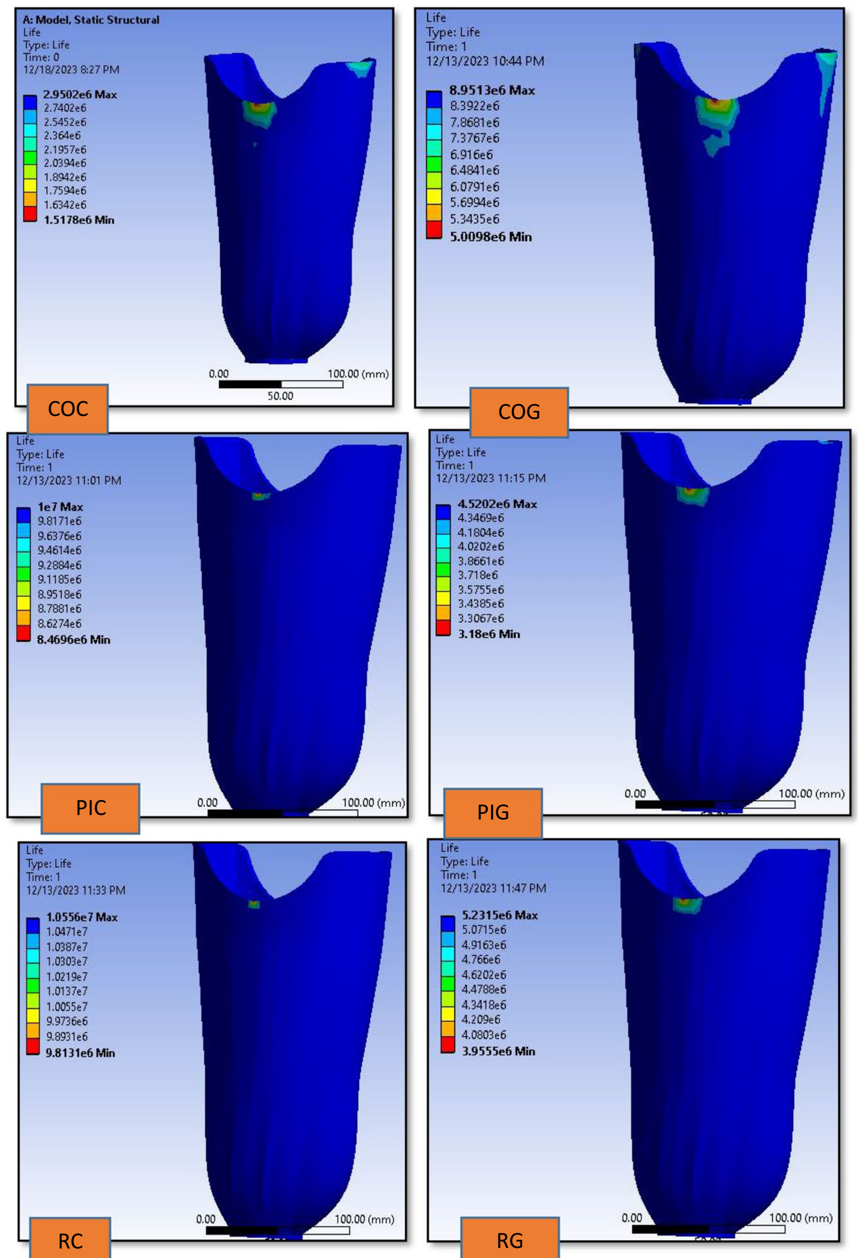

(B)

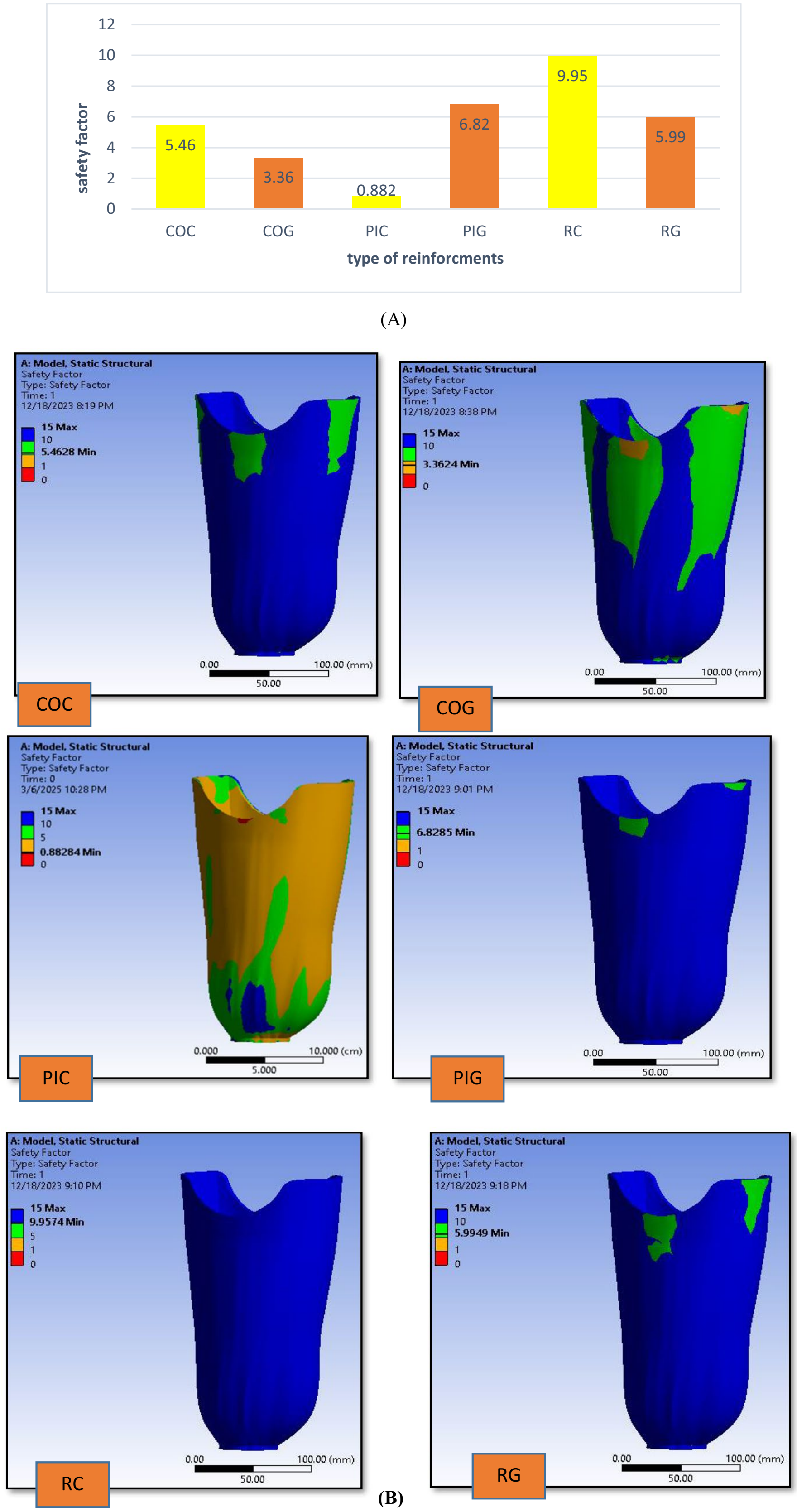

Fig. 10 **A** Numerical results of composites safety factor. **B** Specimens of contours of laminations safety factor

Fig. 11 **A** Numerical equivalent von Mises stress distribution. **B** Analysis of equivalent von Mises stress of the socket

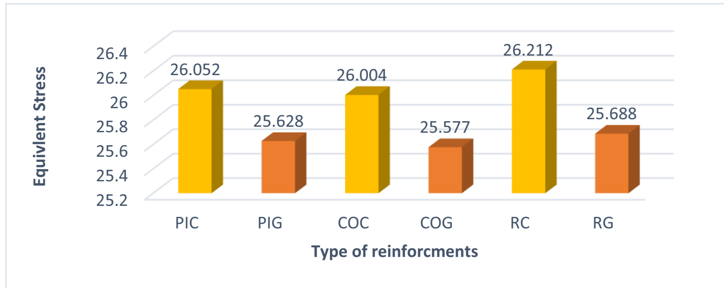

(A)

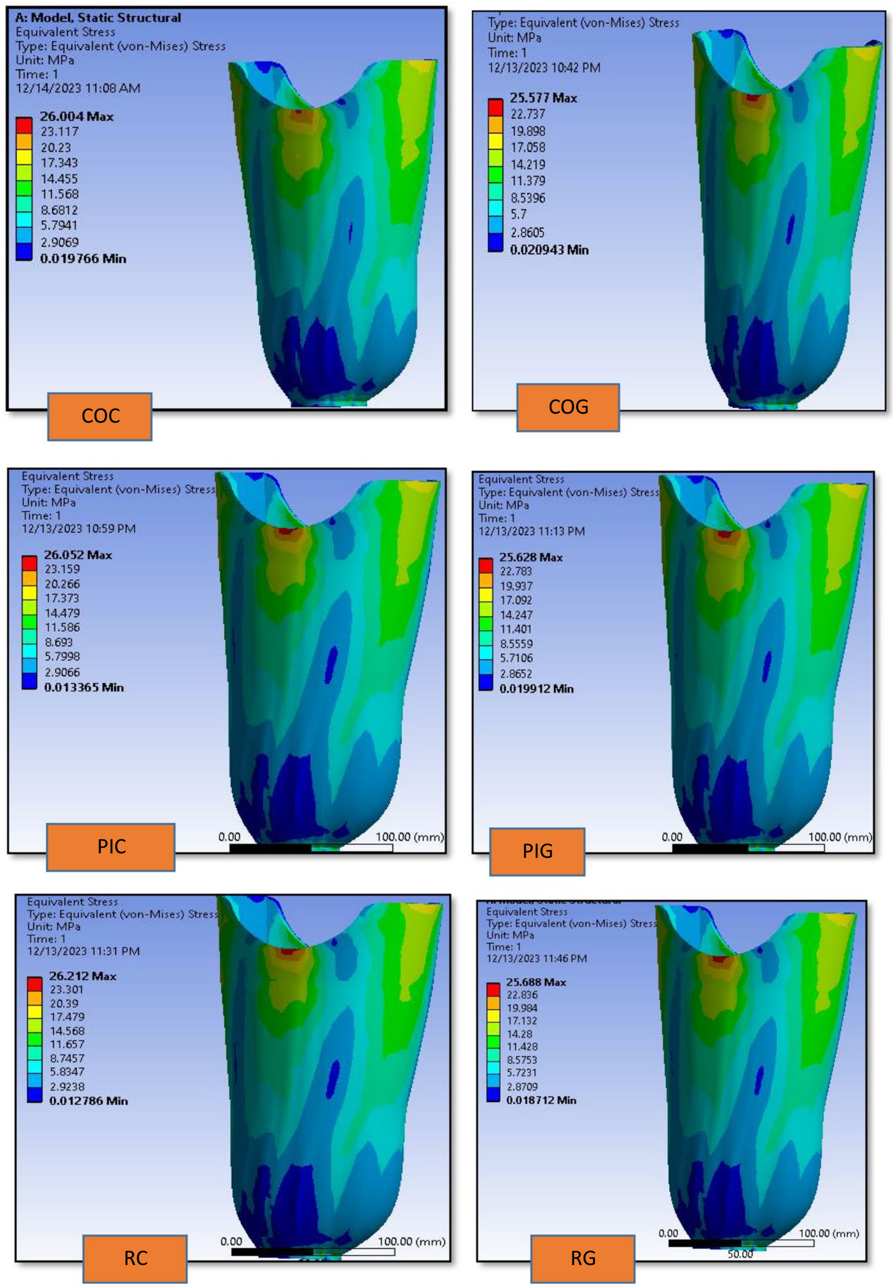

(B)

Fig. 12 **A** Numerical maximum shear stress of laminated groups. **B** Analysis of numerical maximum shear stress of the socket

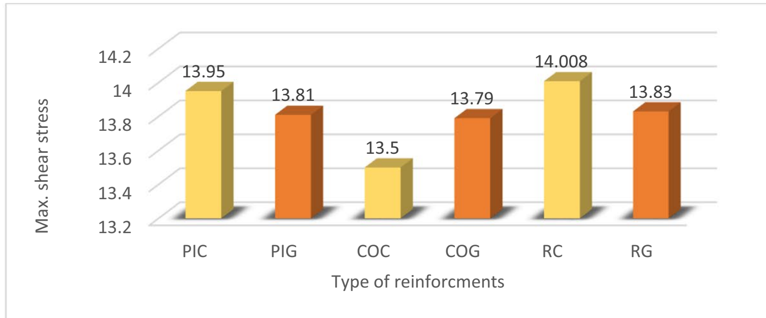

(A)

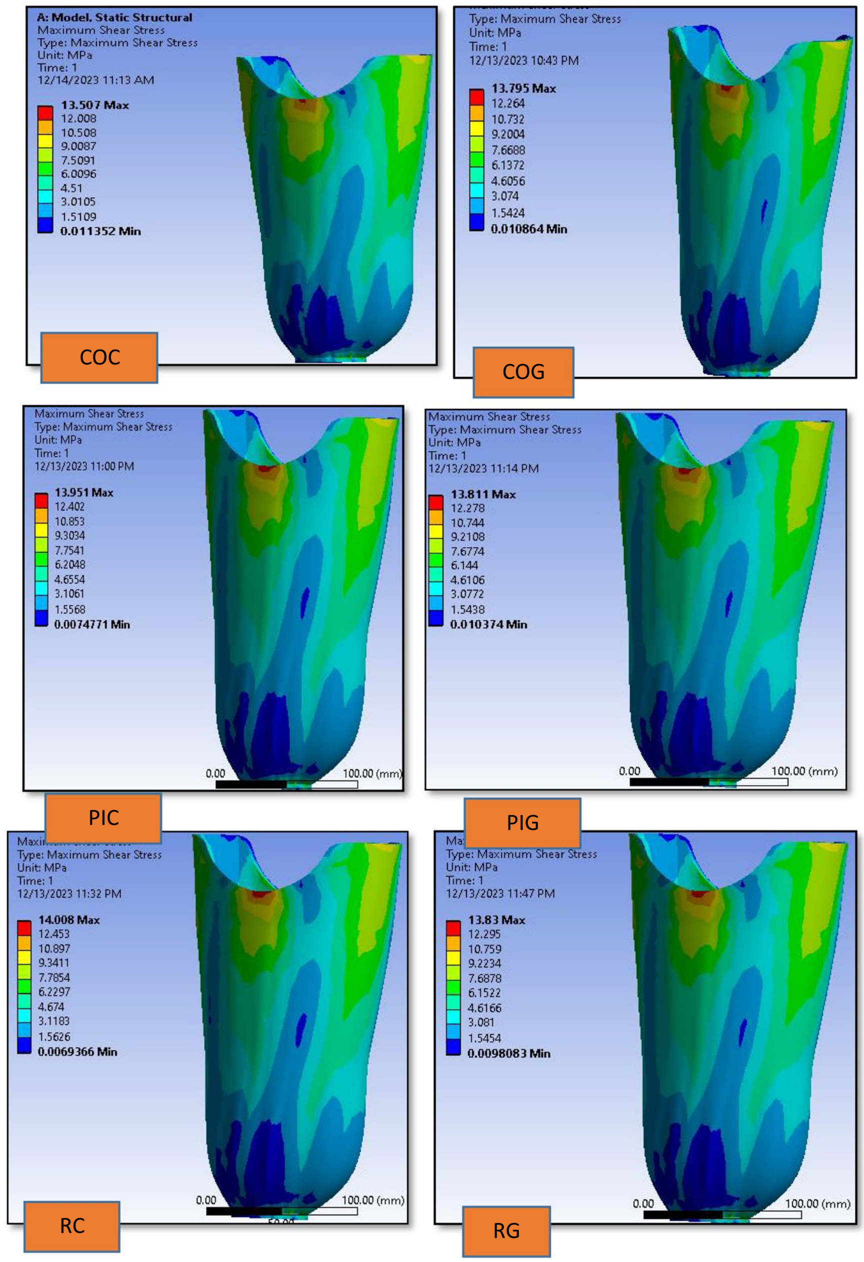

(B)

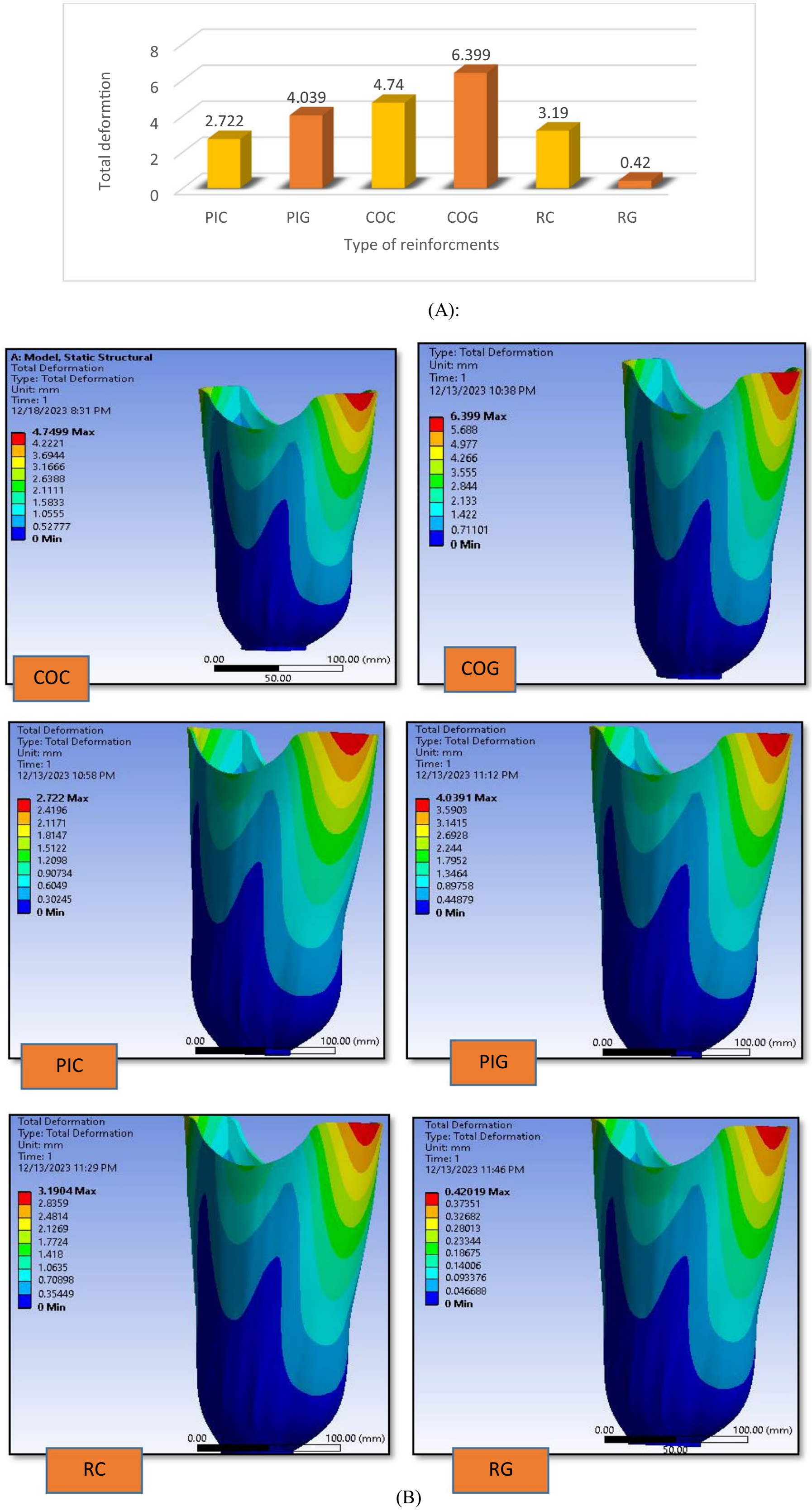

Fig. 13 **A** Numerical total deformation of lamination groups. **B** Contours of total deformation distribution of lamination groups

Fig. 14 Theoretical failure index of different prosthetic composites

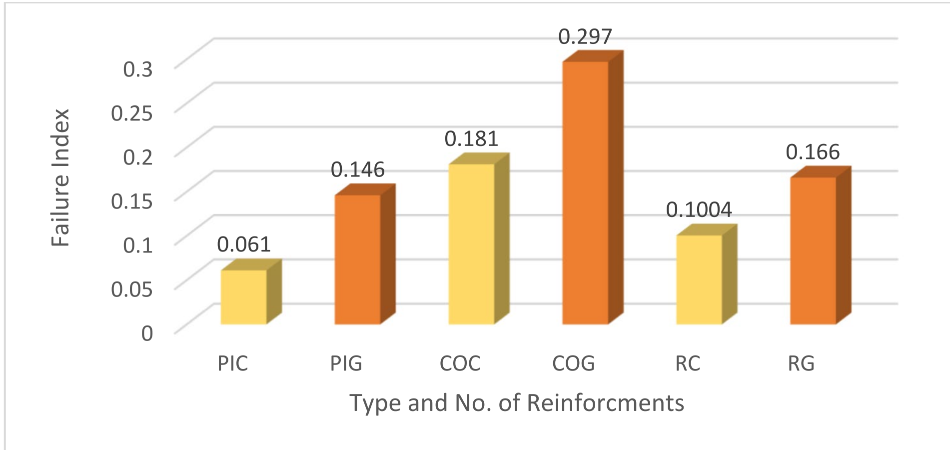

magnitude. The figures show that the uppermost values of maximum shear stress are focused on lateral and basal sockets [50].

Fatigue Total Deformation Results

The findings of the types of reinforcements used in these unique lamination groups and the total deformation obtained for every specimen are shown in Fig. 13A. Lamination 2 has the highest perceptible deformation value at 6.39 mm, while Lamination 4 exhibits the lowest overall deformation at 0.42 mm [52]. It is demonstrated that the deformation value differs according to the kind of reinforcement in various layers. When assessing laminates with an identical number of layers, the deformation in the laminated materials with carbon fiber is lower than the deformation in the laminated materials with glass fiber. The deformation value decreased because of a rise in Young's modulus. Additionally, the material strengthened with natural fibers provides testimony of the deformation significance because carbon fibers have better mechanical properties and can support higher external loads than glass fibers.

It is significant to point out that the socket's deformation numbers are appropriate when utilizing these composites, since, to give the patient's skin convenience, the socket must be deformed within a range of the values above when dispersed on the interface pressure. Conversely, the lowest level originated in the basal plane of the socket [53, 54].

The contour maps of the composites are shown in Fig. 13B, which also indicates the probable position and the amount of total deformation for each lamination group. These plots illustrate the total amount of deformation across the material. These figures show that the lateral plane of the socket contains the greatest values of total deformation, while the base of the socket includes the lowest values of overall deformation [18].

Theoretical Results

Failure Index (K)

Figure 14 illustrates the connection between the kind of reinforcement and the failure index. The whole extent of deformation throughout the material is depicted in these figures. The lateral plane of the socket has the highest values of overall deformation, whereas the base of the socket has the smallest values, as seen in these figures. The hybrid (coir + glass) lamination group showed a higher failure index than the remaining groups with 0.297, which can be explained by the phenomena of thermal cycling that might have resulted in polymer/matrix interface bonding breaking or the composite delaminating [6, 55]. Hybrid (pineapple carbon) showed the lowest, at 0.061, due to carbon fiber's outstanding fatigue qualities and chemical and thermal stability [56].

Factor of Safety (SF)

Figure 15 shows that the theoretical safety factor was acquired fully to understand the newly suggested materials' performance. The (pineapple + carbon) laminated group obtained the highest theoretical safety factor. Because of the remarkable qualities of carbon fiber, the blend of pineapple and carbon fiber produced the best results out of all the laminations. All groups generally demonstrated significant conformance as determined by theoretical and numerical variables. However, lamination with coir natural fiber had the lowest safety factor at 3.36.

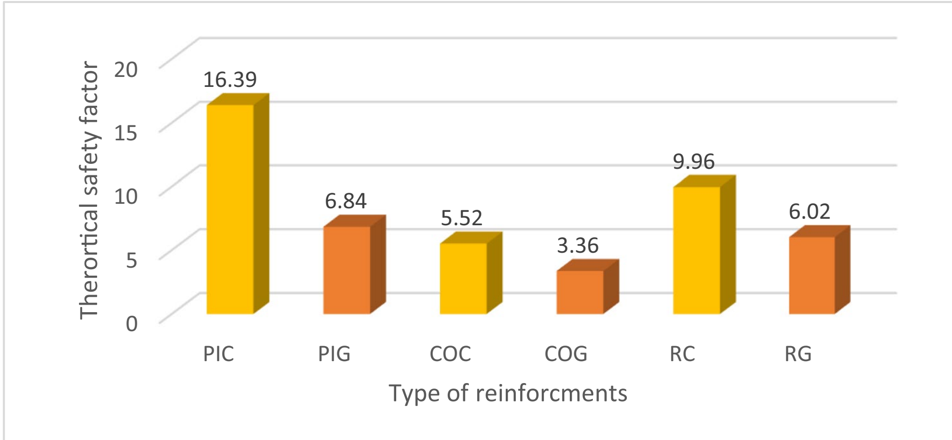

Fig. 15 Theoretical safety factor of prosthetic socket lamination samples

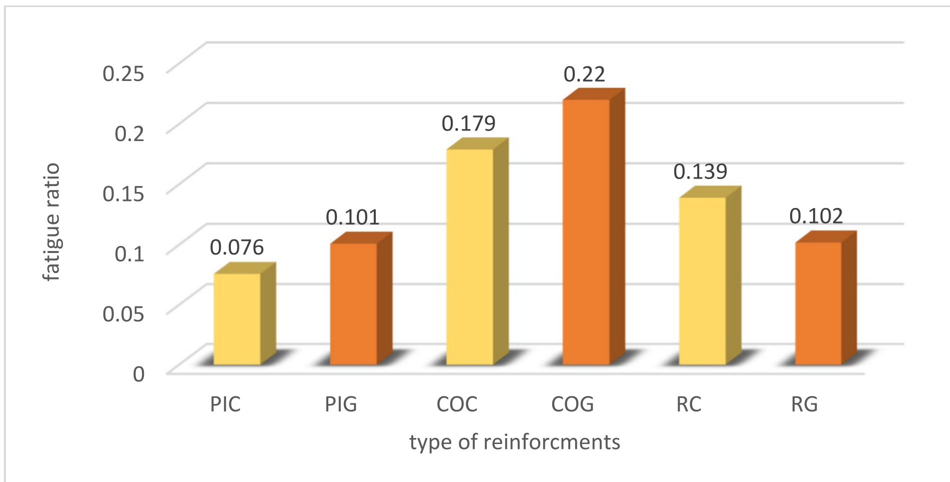

Fig. 16 Theoretical fatigue ratio of prosthetic socket lamination samples

This could indicate that a part or structure may not be able to sustain any further load when the design load is met and could gradually fail [57, 58].

Fatigue Ratio (Rf):

Figure 16 illustrates the connection between the kind of reinforcement and the fatigue ratio; the results clearly show that the composite with the glass reinforcement and coir had the greatest fatigue ratio, at 0.22. The hybrid (coir + glass) lamination group showed a higher fatigue ratio than the remaining group, and this can be explained by the fact that natural coir fiber has the lowest mechanical characteristics, in addition to poor contact bonding at the interface between fiber and matrix. These materials' tensile strength and fatigue limit match the experimental findings [59, 60, and 61].

Limitations and Future Scope of the Study

Information access is limited, and time is restricted. However, examining the mechanical properties of several naturally enhanced composites and analyzing finite elements on many models with varying genders, maturity, and amputations is possible.

Conclusions

As an alternative to traditional and artificial composites in the prosthesis socket production method, natural fiber–strengthened composites can offer lighter substances with more specific strength, stiffness, security, and environmental sustainability. These materials have more possibilities for usage in mild load-bearing and structural applications. The following is a summary of the main conclusions: rami fiber–reinforced composites are the best option to enhance the fatigue properties of a prosthetic socket since they produce the best experimental, numerical, and theoretical findings. Thermal degradation from the specimen's self-heating and micromechanical degradation (crack formation and progression) from repeated loading are the main causes of fatigue damage in coir fiber–reinforced polymer matrix composites. A material with good mechanical qualities must be utilized because these features strongly influence the fatigue life of a prosthesis. Because of its mechanical and physical attributes, employing woven carbon fiber cloth is beneficial. The prosthetic sockets are secure if they have a minimal factor of safety of 3.36, which was determined by fatigue analysis utilizing the suggested material. The fatigue attributes of laminated composites were evaluated using an experimental technique that demonstrated excellent agreement with numerical fatigue findings.

Acknowledgements The researchers express their gratitude to the entire faculty of Engineering at the University of Technology.

Author Contribution Material preparation, data collection, and analysis were performed by Noor Faheed and Mahmood Mahmood. The first draft of the manuscript was written by Rasha Issa, Qahtan Adnan, and Dheyaa S. J. Al-saedi, who commented on previous versions. The authors read and approved the final manuscript.

Data Availability It was formed through the investigation as a result of a data-sharing order that is available on an open basis and does not conflict with datasets with DOIs.

Declarations

Ethical Approval The authors declare that there was no human or animal involvement in the research.

Conflict of interest The authors declare no competing interests.

References

1. World Health Organization. It is standards for prosthetics and orthotics. Geneva, Switzerland: WHO; 2017.
2. Hughes J. Biomechanics of the through-knee prosthesis. Prosthet Orthot Int. 1983;7(2):96–9.
3. Pinzur MS, Gold J, Schwartz D, Gross N. Energy demands walking in dysvascular amputees as related to the level of amputation. Orthopedics. 1992;15(9):1033–7.
4. Penn-barwell JG. Outcomes in lower limb amputation following trauma: a systematic review and meta-analysis. Injury. 2011;42(12):1474–9.
5. Panhelleux B, Shalhoub J, Silverman AK, McGregor AH. A review of through-knee amputation. Vascular. 2022;30(6):1149–59.
6. Hamad QA, Al-Hasani FJ, Faheed NK. Comparative study of biotin and hydroxyapatite on biological properties of the composite coating. Int J Biomater. 2022;2022(1):8802111.
7. Al-Kaisy HA, Issa R, Faheed NK. Enhancing the biocompatibility of titanium implants with chitosan-alginate bio-composite coatings reinforced with HAP and ZnO. Rev Compos Mater Av. 2024;34(2):125–32.
8. Faheed NK, Hamad QA, Oleiwi JK. Tensile and stress analysis of hybrid composite prosthetic socket reinforced with natural fibers. J Renew Mater. 2022;10(7):1989–2013.
9. Faheed NK, Hamad QA, Oleiwi JK. Enhancement of the flexural and impact properties of laminated biocomposite by new natural fibers for artificial lower limb socket. Adv Mater Process Technol. 2022;8(4):4347–64.
10. Santulli C. Mechanical and impact damage analysis on carbon/natural fibers hybrid composites: a review. Materials. 2019;12(3):517.
11. Faheed NK, Hamad QA, Issa RAH. Investigation of the effect of thermal, mechanical, and morphological properties of bio-composites prosthetic socket. Compos Interfaces. 2023;31(3):331–55.
12. Al-Hasani FJ, Hamad QA, Faheed NK. Enhancing the alginate-based composite layer's cell viability and antibacterial properties by adding active particulates. Discov Appl Sci. 2024;6(2):70.
13. Faheed NK. Advantages of natural fiber composites for biomedical applications: a review of recent advances. Emergent Matt. 2024;7:63–75. https://doi.org/10.1007/s42247-023-00620-x.
14. Hamad QA, Oleiwi JK, Abdulrahman SA. Tensile properties of laminated composite prosthetic socket reinforced by different fibers. Mater Today Proc. 2021;80:2353–9.
15. Campbell AI, Sexton S, Schaschke CJ, Kinsman H, McLaughlin B, Boyle M. Prosthetic limb sockets from plant-based composite materials. Prosthet Orthot Int. 2012;36:181–9.
16. Faheed Noor K, Oleiwib Jawad K, Hamad Qahtan A. Effect of different fiber reinforcements on some properties of prosthetic socket. Eng Technol J. 2021;39(11):1715–26.
17. Al-Khazraji K, Kadhim J, Ahmed PS. Tensile and fatigue characteristics of lower-limb prosthetic socket made from composite materials. In: Proceedings of the 2012 international conference on industrial engineering and operations management Istanbul. Turkey; 2012. pp. 847–852.
18. Sattar MA, Ghazwan A, Abbas SM. Study and analysis of the mechanical properties and pressure socket for through-knee amputation. Int J Adv Technol Eng Explor. 2023;10(105):1063.
19. Oleiwi JK, Hamad QA, Faheed NK. Experimental, theoretical, and numerical analysis of laminated composite prosthetic socket reinforced with flax and cotton fibers. Biotribology. 2023;1(35):100244.
20. Khatun MF, Sultana S, ParvinNur H, et al. Physical, mechanical, thermal, and morphological analysis of date palm mat (DPM) and palmyra palm fruit (PPF) fiber-reinforced high-density polyethylene hybrid composites. Adv Mater Sci. 2019;4(2):1–6.
21. Appadurai M, Jenish I, Sahayaraj AF, Irudaya Raj EF, Suresh P. Sea sand abrasive wear of red mud micro-particle reinforced Cissus quadrangularis stem fiber/epoxy composite. J Nat Fibers. 2022;19(16):1–16.
22. Standard test method for tensile properties of plastics D638–03. Annual Book of ASTM Standards. New York; 2004. pp. 1–17. http://www.ansi.org.
23. Standard test method for fatigue testing of plastics ASTM E606-98. Annual Book of ASTM Standards. New York; 1998. pp. 1–15. https://www.ansi.org.
24. Resan KK, Zeki A. Design and analysis of knee ankle foot orthosis (KAFO) for a paraplegic person. Eng Technol J. 2013;31(8):1521–33.
25. Kadhim FM, Takhakh AM, Chiad JS. Vibration Measurement and analysis of knee, ankle foot orthosis for metal and plastic KAFO type. ASME Int Mech Eng Congress Expos. 2013;56222:1–11.
26. Ansys-11 Workbench help guide, SAS IP, Inc., Eleventh Edition; 2008. pp. 1–286. http://www.ansys.com.

27. www.maelabs.ucsd.edu/.../Materials/.../solutions/MESPD-Solution-manual. pdf. "Materials: engineering, science, properties, and design solution manual", (2010).
28. Clifford MM. Case studies in engineering design. John Wily Publishing Ltd.; 1998. pp. 1–272. https://www.amazon.com/Studies-Engineering-Design-Cliff-Matthews/dp/0340691352.
29. www.webs1.uidaho.edu/Fatigue Analysis of Combined Loading Mode. 2010.
30. Mustafa TI, Muhsin JJ, Resan KK. Study of creep-fatigue interaction in the prosthetic socket below knee. Innov Syst Des Eng. 2013;4(5):383–94.
31. Ju Q, S. Ion S. A failure criterion revision method for composite materials. Polym Polym Compos. 2021;29(7):854–62.
32. Kim JK, Kim HS, Lee DG. Investigation of optimal surface treatments for carbon/epoxy composite adhesive joints. J Adhes Sci Technol. 2003;17(3):329–52.
33. Kadhim FM, Chiad JS, Takhakh AM. Design and manufacturing knee joint for smart transfemoral prosthetic. IOP Conf Ser: Mater Sci Eng. 2018;454(1):012078.
34. Ismail MR, Al-Waily M, Kadhim AA. Biomechanical analysis and gait assessment for normal and braced legs. Int J Mech Mechatron Eng. 2018;18(03):1–9.
35. Abbas BR, Hebeatir KA, Resan KK. Effect of CO2 laser on some properties of NI46TI50CU4 shape memory alloy. Int J Mech Prod Eng Res Dev. 2018;08(02):451–60.
36. Jones RM. Mechanics of composite material". New York: McGraw-Hill; 1975.
37. Groover MP. Fundamentals of modern manufacturing materials, processes, and systems. 4th ed. John Wiley & Sons, Inc.; 2019. pp. 1–1024. https://www.amazon.com/Fundamentals-Modern-Manufacturing-Materials-Processes/dp/0470467002.
38. Elie SM. Study of mechanical properties and thermal conductivity for polymer composite material reinforced by aluminum and aluminum oxide particles. M.Sc: Thesis, University of Technology, Baghdad, Iraq; 2007.
39. NoorunnisaKhanam P, Abdul Khalil HPS, Jawaid M, Ramachandra Reddy G, Surya Narayana C, Venkata Naidu S. Sisal/carbon fibre reinforced hybrid composites: tensile, flexural and chemical resistance properties. J Polym Environ. 2010;18:727–33.
40. Jweeg M. Dynamic analysis of stiffened and unstiffened composite plates. Iraqi J Mech Mater Eng. 2013;13(4):689–713.
41. Njim EK, Al-Waily M, Bakhy SH. A review of the recent research on the experimental tests of functionally graded sandwich panels. J Mech Eng Res Dev. 2021;44(3):420–441.
42. Shahzad A. Investigation into fatigue strength of natural/synthetic fiber-based composite materials. Woodhead Publishing Series in Composites Science and Engineering; 2019. pp. 215–239. https://doi.org/10.1016/B978-0-08-102292-4.00012-6.
43. Al-Shroofy MN, Hamad QA, Faheed NK, Al-Kaisy H. Evaluation of novel chitosan-based composites coating on wettability for pure titanium implants. J Renew Mater. 2023;11(4):1601–12. https://doi.org/10.32604/jrm.2023.023213.
44. Hamad QA, Faheed NK, Issa RAH. Wettability, morphological, miscibility characterization of alginate, and chitosan-based biocomposite coatings. Surface Eng. 2024;40(5):629–47.
45. Bhowmik S, Kumar S, Mahakur VK. Various factors affecting the fatigue performance of natural fiber-reinforced polymer composites: a systematic review. Iran Polym J. 2024;33(2):249–71.
46. Shahzad A. Impact and fatigue properties of natural fiber composites. Ph.D. Thesis, Swansea University, United Kingdom of Great Britain; 2009. p. 399. https://cronfa.swan.ac.uk/Record/cronfa43056.
47. Miller BA. Failure analysis and prevention, fatigue failures. ASM Int Handbook. 2002;11:58.
48. Kohnke P. Ansys-11 Workbench help guide, SAS IP, Inc. 11th ed; 2008. pp. 1–268. http://www.ansys.com.
49. Nachippan NM, Alphonse M, Raja VB, Palanikumar K, Kiran RSU, Krishna VG. Numerical analysis of natural fiber reinforced composite bumper. Mater Today: Proc. 2021;46:3817–23.
50. Oleiwi JK, Alwan MK, Hamad QA. Numerically and experimentally studying of some mechanical properties of the polyester matrix composite material reinforced by jute fibers. Eng Tech J. 2014;32(9):2235–2247. https://doi.org/10.30684/etj.32.9A11.
51. Islam MZ. Fatigue behavior of flax fiber reinforced polymer matrix composites. MSC Thesis, North Dakota State University, USA; 2019. pp. 1–59. https://library.ndsu.edu/ir/items/6a2b027c-6f21-4085-8677-6bfc6aa896f2.
52. Bolten W. Engineering materials technology. Third edition, Butterworth & Heinemann publishing Ltd.; 1998. pp. 1–480. https://www.amazon.com/Engineering-Materials-Technology-Third-Bolton/dp/0750639172.
53. Hamad QA, Rahman HJA, Faheed NK. Improving some mechanical properties of green biocomposite by natural pumpkin powders for prosthetic socket. In AIP Conf Proc. 2023;2787(1):020024–10. https://doi.org/10.1063/5.0149834.
54. www.webs1.uidaho.edu/"Fatigue analysis of combined loading mode", 2010.
55. Koch I, Zscheyge M, Tittmann K, Gude M. Numerical fatigue analysis of CFRP components. Compos Struct. 2017;168:392–401.
56. Ibraheem B, Salman SF, Ali AH. Numerical analysis of fatigue life and strength of AA5052 aluminum alloy reinforced with ZrO2, TiO2 and Al2O3 nanoparticles. Diyala J Eng Sci. 2022;15(2):83–93.
57. AL-Bedhany J, Legutko S, AL-Maliki A, Mankhi AT. A new theory of damage estimation and fatigue life prediction. Misan J Eng Sci. 2023;2(2):1–11. https://doi.org/10.61263/mjes.v2i2.26.
58. Faheed NK, Issa RAH, Hamad QA. A review on durability of high-performance cellulose-based biocomposites. Nanosci Technol: Int J. 2024;15(4):97–118. https://doi.org/10.1615/NanoSciTechnolIntJ.v15.i4.60.
59. Majeed IH. Experimental and numerical study of torsional solid and hollow section of polyolefin fiber-reinforced concrete beams. Misan J Eng Sci. 2023;2(2):71–84. https://doi.org/10.61263/mjes.v2i2.63.
60. Faheed NK, Oleiwi JK, Hamad QA. Effect of weathering on some mechanical properties of prosthetic composites. Mater Today: Proc. 2022;57:422–30.
61. Al-Lami H, Al-Saedi DSJ, AlMaidib AAH, Al-Yasiri Q. Conjoint effect of nanofluids and baffles on a heat exchanger thermal performance: numerical approach. Misan J Eng Sci. 2024;3(2):137–55. https://doi.org/10.61263/mjes.v3i2.105.

Publisher's Note Springer Nature remains neutral with regard to jurisdictional claims in published maps and institutional affiliations.